



Tunneling spectroscopy of bound and resonant states in superconducting proximity structures

Y. Levi^a, O. Millo^{a,*}, N.D. Rizzo^b, D.E. Prober^b, L.R. Motowidlo^c

^a *Racah Institute of Physics, the Hebrew University, Jerusalem 91904, Israel*

^b *Applied Physics, Yale University, New Haven, CT 06520-8284, USA*

^c *IGC-AS, Waterbury, CT 06704, USA*

Abstract

Scanning tunneling microscopy and spectroscopy are employed in order to map with nanometer resolution the local quasi-particle density of states in superconducting proximity structures. Our experimental configuration is unique, in that the tunneling current flows in parallel to the interfaces between different materials. We focus here on the measurement of bound and resonant states, arising from multiple Andreev reflections of quasi-particles propagating in a plane perpendicular to the tunneling current. © 1999 Elsevier Science B.V. All rights reserved.

Keywords: Scanning tunneling microscopy; Superconductivity; Superconductor—metal interfaces

1. Introduction

The mutual influence of a superconductor (S) in electrical contact with a normal metal (N), a phenomenon known as the proximity effect (PE), has been studied extensively in the past three decades [1,2]. Central issues of the PE are the spatial variations of the local quasi-particle density of states (DOS) in the vicinity of the N–S boundary [3], and the presence of quasi-particle bound and resonant states. Recently, research of the PE gained further momentum thanks to technological advances that enable the fabrication of complex mesoscopic devices. Nevertheless, many of these works [4–6] followed earlier studies [2] and addressed macroscopic properties of the samples, thus obtaining average

rather than local information. In other cases [7] spatially resolved data were sought, but only in a limited number of locations. Scanning tunneling microscopy (STM) can be very effective in the research of PE, since the DOS can be measured locally. At $T = 0$, the tunneling dI/dV vs. V curve is directly proportional to the sample's DOS, while at finite temperatures it is thermally smeared. By taking topographic images simultaneously with tunneling current–voltage (I – V) or dI/dV vs. V characteristics, one obtains a spatially resolved map of the DOS. Some STM experiments treated systems composed of a normal metal island film deposited onto a S substrate [8–10] so that tunneling took place *perpendicular* to the S–N interface. Hess et al. measured a type-II superconductor in the Abrikosov vortex lattice state, mapping the DOS around and within a single flux-vortex [11,12]. However, this study did not address a structure involving *different* metals.

* Corresponding author. Tel.: +972-2-658-5670; Fax: +972-2-658-4437; E-mail: milode@vms.huji.ac.il

In our research we employ a cryogenic STM to measure with nanometer spatial resolution the local quasi-particle DOS, when tunneling *parallel* to the material boundaries. The samples consist of ordered arrays of S and N filaments of ‘semi-infinite’ length in electrical contact, having a lateral scale in the sub-micron range. This scale is suitable for STM measurements of mesoscopic effects resulting from multiple Andreev reflections. An illustration of the experimental configuration is shown in Fig. 1(a). In

previous publications [13,14] we focused on the evolution of the DOS as a function of distance from the S–N boundary, mainly the suppression of the superconducting gap in S and its penetration into N. The effect of the ferromagnetic Ni (inimical to S), present in some of the samples, was also addressed.

In this paper we report evidence of de Gennes–Saint James bound states [2,15] and Tomasch oscillations [2,16] (manifesting resonant states), observed at specific STM tip positions over the sample. These measurements are unique in that tunneling occurs perpendicular to the plane where the quasi-particles which undergo Andreev reflections propagate (and in parallel to the reflecting planes).

2. Experimental

The samples studied are ‘artificial pinning centers (APCs) wires’ manufactured at IGC-Advanced Superconductors. APC superconducting wires are engineered to enhance magnetic flux pinning in order to increase the critical current at high magnetic fields. In this approach chosen pin materials are introduced in a well defined ordered filamentary configuration. These wires have already demonstrated better performance than those produced with conventional processing [17].

We used two types of APC wires. The first, sample A, has the ‘island’ pin geometry and uses a Cu-coated Ni pin; (the Cu sleeve serves as a diffusion barrier against the migration of Ni into NbTi). The ‘unit filament’ consists of a pin placed inside a NbTi (S) cylinder that is surrounded by a thin Nb cylinder [S’ in Fig. 2(a)]. The unit filament has an outer diameter of 1.3 μm , and the pin comprises of a cylindrical Ni filament 200 nm in diameter, surrounded by a 50 nm thick Cu sleeve. A SEM micrograph taken on sample A displaying part of an array of individual Ni island pins is shown in Fig. 1(b). The second wire, sample B, has the ‘barrier-pin’ geometry, where the unit filament is a NbTi hexagon 80 nm in size, surrounded by a 15 nm thick Cu cladding (the pin), making the distance between adjacent superconducting filaments 30 nm.

Sample preparation for STM measurements consists of cutting the wires, polishing them along their

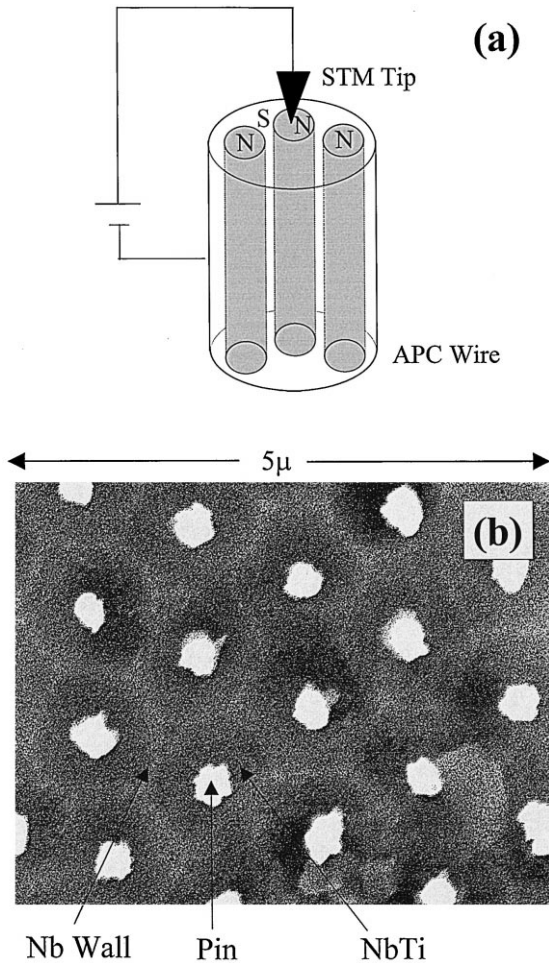


Fig. 1. (a) Schematic of the experimental setup. The black arrow represents the STM tip, and tunneling takes place in parallel to the interfaces between the wire's constituents. (b) SEM micrograph of the large Ni island-pin wire, sample A, displaying an array of unit filaments. Each unit filament consists of a pin (bright), surrounded by a NbTi hexagon (dark) that is coated by a thin Nb layer (bright).

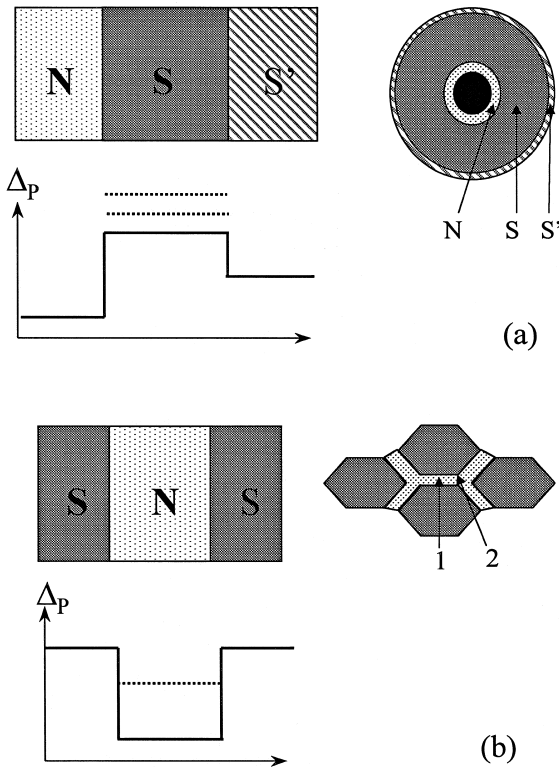


Fig. 2. (a) Left: an illustration of the variation of the pair-potential Δ_p at the boundaries between different materials. Such a configuration can give rise to resonant states (dashed lines) resulting in Tomasch oscillations. Right: schematic of the Ni island-pin unit filament, where this configuration is realized; N(Cu), S(NbTi), S'(Nb). (b) Left: an illustration of the variation of the pair-potential Δ_p in a SNS structure. This configuration can support quasi-particle bound states (dashed line). Right: a schematic of the unit filament in the Cu barrier-pin wire, where such a configuration is realized; N(Cu), S(NbTi).

cross-section and finally subjecting them to a short chemical etch. Immediately afterwards the samples are mounted onto our cryogenic STM, having a Pt-Ir (normal alloy) tip. All the data presented in this paper were acquired at a temperature of 4.2 K.

STM topographic images of the wire cross-section were taken simultaneously with I - V characteristics at different lateral tip positions. The I - V curves were acquired while momentarily disabling the STM feedback loop. dI/dV vs. V (differential conductance) curves were either measured directly using standard lock-in technique, or by numerical differentiation of the acquired I - V curves. Care was taken

to use small enough tunneling currents so that local superconductivity, in particular the measured DOS, was unaffected.

3. Results and discussion

Our samples consist of a multitude of S-N interfaces. Such a configuration may support, in favorable cases, quasi-particle bound and resonant states, resulting from multiple Andreev reflections. When a superconductor is placed in between two materials having a pair potential [1,2] Δ_p , smaller than its own, the structure results in a pair potential mesa. Quasi-particles in the superconductor having energies above the pair potential may undergo double Andreev reflections at opposing boundaries. This can give rise to resonant states, reflected in the dI/dV vs. V curves as Tomasch oscillations [2,16]. Theoretical calculations yield the energy $E_n^2 \approx \Delta_p^2 + (hv_F/2d_S^2n^2)$ for the n th conductance peak, in a one-dimensional structure. d_S and Δ_p are the width of the superconductor and its pair potential, respectively. v_F is the renormalized (due to strong coupling effects) Fermi velocity in the superconductor, $\sim 10^8$ cm/s in NbTi [2].

A case of Tomasch oscillations appears in the Ni island-pin wires, as sketched in Fig. 2(a). The thick NbTi cylinder is placed between the inner Cu sleeve and the outer Nb layer. Andreev reflections can then take place at the Cu-NbTi and NbTi-Nb interfaces. Although Nb and NbTi have a similar T_C , Δ_p of NbTi is larger due to strong coupling effects [2]. Fig. 3(a) presents a differential conductance curve taken on sample A, when the tip was placed over the NbTi near the NbTi-Cu boundary. Tomasch oscillations, comprising the above-gap structure in the curve, are clearly visible both at positive and at negative biases, while no sub-gap structures are present.

These oscillations cannot be attributed to phonon structure, which is found in NbTi only at energies above 10 meV [2]. Nevertheless, in order to prove that they are indeed due to resonant states, we plot in the inset of Fig. 3(a) the square of the conductance-peak energies (E_n^2) vs. n^2 . The data can be well fit to a straight line, from which Δ_p and the width of the superconductor are extracted, using the equation above. For the data presented here these values are

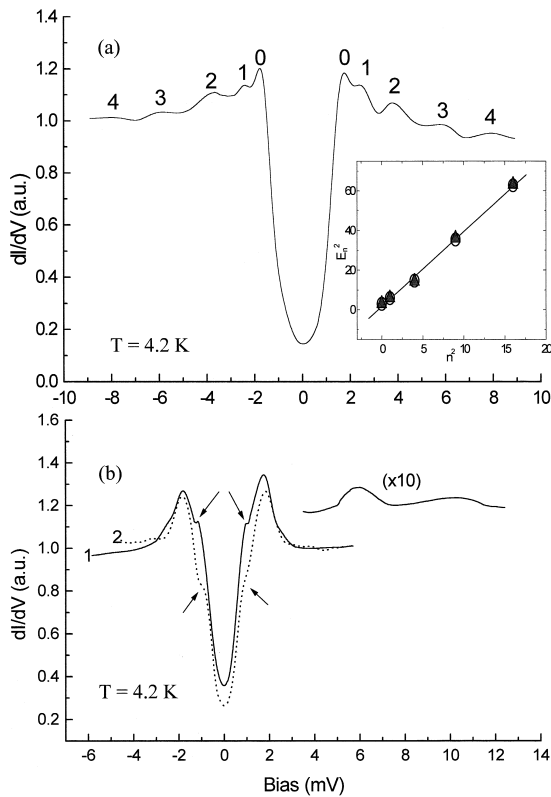


Fig. 3. (a) A dI/dV vs. V curve taken on the Ni island-pin wire, sample A, with the STM tip situated on the NbTi, in the vicinity of the Cu–NbTi interface. Notice the four peaks above the gap edge ('0'), attributed to Tomasch oscillations. Inset: The energy squared of the peak positions plotted as a function of the square of peak number. The nearly overlapping symbols correspond to peaks at negative (circles) and positive (triangles) bias. The data points fall on a straight line, from which we obtain $\Delta_p = 1.3$ meV nm and $d_s = 510$ nm. (b) Two normalized dI/dV vs. V curves taken on a Cu barrier-pin wire, on the Cu, in the vicinity of the NbTi–Cu interface. The curves were acquired at two different positions, as indicated in Fig. 2(b). Both curves exhibit a sub-gap structure (highlighted by arrows) corresponding to bound states. The above-gap part of curve #1 (magnified tenfold) exhibits two Tomasch oscillations.

$\Delta_p = 1.3$ meV and $d_s = 510$ nm, and in all the other conductance curves that exhibited Tomasch oscillations, taken on different wires of this type at various locations, we found $1.2 \leq \Delta_p \leq 1.8$ meV and $490 \leq d_s \leq 520$ nm. These values of Δ_p are consistent with those reported in the literature [2], and those of d_s are in close agreement with the nominal thickness of NbTi in this sample, 500 nm. Further evidence that supports the assignment of the above-gap structure to

Tomasch oscillations is that they could be observed only in the NbTi, but not inside the Cu. Moreover, these oscillations were not seen deep inside the S, but only *near* the S–N boundary, where Andreev reflections take place. In sample B we could find evidence only for the two lowest resonant states. This is because here the thickness of S is smaller, shifting the resonances towards higher energies, where the probability to undergo Andreev reflections is much smaller. These oscillations can be seen in Fig. 3(b), detached from the rest of the curve, due to a 10-fold magnification that was required in order to observe them. The clear observation of Tomasch oscillations in our sample is not trivial. Electrons probably do not travel ballistically across the 500 nm thick NbTi cylinder, as assumed in the conventional model. However, at 4.2 K quasi-particles travel phase coherently across the NbTi and elastic scatterings don't alter their path considerably, conditions that seem to be sufficient for the detection of Tomasch oscillations.

Next we discuss the quasi-particles bound states. When a normal metal is placed in between two superconductors, a pair-potential well which may support one or more quasi-particle bound states is formed [2,15]. This is the situation in the Cu barrier pin wire, as sketched in Fig. 2(b). It can be shown [2] that in the simplest one dimensional case the energy of the n th bound state E_n is given by $(2d_N/\hbar v_F)E_n = n\pi + \cos^{-1}(E_n/\Delta_p)$ where d_N is the width of the normal region. Fig. 3(b) depicts two differential conductance curves taken on the wire with the Cu barrier pin, sample B, over the Cu near the Cu–NbTi boundary. The first curve was acquired in the middle of a hexagon's side while the other was acquired near a corner, as is illustrated in Fig. 2(b). We see that both curves have almost the same gap and manifest a sub-gap structure, which we attribute to bound states. It should be noted that the curves taken in the middle of a hexagon's side [#1 in Fig. 2(b) and Fig. 3(b)] exhibit a sharper and somewhat higher energy of the bound state than those taken at the corner (#2). The reason for this may be that at the corner d_N is not as well defined as in the middle of a side section. Furthermore, while the bound state observed in curve #1 results predominantly from Andreev reflections *perpendicular* to the Cu channel, those in curve #2 have contribu-

tions from reflections of quasi-particles traversing *along* the channel. This leads to both broadening and lowering of the bound states in the corner position. The energies of the sub-gap features are somewhat lower, although in reasonable agreement with theoretical predictions for our sample's parameters. We wish to note that despite these spatial variations in the detailed shape of the sub-gap structure, such structures have been found *only inside* the Cu region. Moreover, even there, they could be resolved only in the vicinity of the S–N boundaries, since deeper inside the Cu the superconductor gap in the DOS masks and overlaps the bound state [13,14]. Nevertheless, wherever it can be detected, the energy of the subgap structure does not depend on the distance from the N–S boundary.

4. Summary

In this work we have employed a cryogenic STM in order to study the bound and resonant states present in N–S proximity structures. In our unique experimental configuration, tunneling took place in parallel to the N–S boundaries, so that the tunneling current was perpendicular to the path of the Andreev-reflected quasi-particles. In this way, the direct effect of coherent multiple Andreev reflections on the local DOS can be measured.

References

- [1] G. Deutscher, P.G. de Gennes, in: R.D. Parks (Ed.), Superconductivity, Vol. 2, Dekker, New York, 1969.
- [2] E.L. Wolf in: Principles of Electron Tunneling Spectroscopy, Oxford, Oxford, 1989.
- [3] W. Belzig, C. Bruder, G. Schoen, Phys. Rev. B 54 (1996) 9443.
- [4] A.C. Mota, P. Visani, A. Pollini, K. Aupke, Physica B 197 (1994) 95.
- [5] L. Capogna, M.G. Blamire, Phys. Rev. B 53 (1996) 5683.
- [6] H. Courtois, Ph. Gandit, D. Mailly, B. Pannetier, Phys. Rev. Lett. 76 (1996) 130.
- [7] S. Gueron, H. Pothier, N.O. Birge, D. Esteve, M.H. Devoret, Phys. Rev. Lett. 77 (1996) 3025.
- [8] S.H. Tessmer, D.J. Van Harlingen, J.W. Lyding, Phys. Rev. Lett. 70 (1993) 3135.
- [9] S.H. Tessmer, M.B. Tarlie, D.J. Van Harlingen, D.L. Maslov, P.M. Goldbart, Phys. Rev. Lett. 77 (1996) 924.
- [10] J. Wildoer, PhD Thesis, TU Delft, 1996.
- [11] H.F. Hess, R.B. Robinson, R.C. Dynes, J.M. Valles Jr., J.V. Waszczak, Phys. Rev. Lett. 62 (1989) 214.
- [12] H.F. Hess, R.B. Robinson, R.C. Dynes, J.M. Valles Jr., J.V. Waszczak, J. Vac. Sci. Technol. A 8 (1990) 450.
- [13] Y. Levi, O. Millo, N.D. Rizzo, D.E. Prober, L.R. Motowidlo, Appl. Phys. Lett. 72 (1998) 480.
- [14] Y. Levi, O. Millo, N.D. Rizzo, D.E. Prober, L.R. Motowidlo, Phys. Rev. B (1999) in press.
- [15] P. G de Gennes, D. Saint James, Phys. Lett. 4 (1963) 151.
- [16] W.J. Tomasch, Phys. Rev. Lett. 15 (1965) 672.
- [17] N.D. Rizzo, J.Q. Wang, D.E. Prober, L.R. Motowidlo, B.A. Zeitlin, Appl. Phys. Lett. 69 (1996) 2285.